Eur. Phys. J. D **28**, 447–451 (2004)
DOI: 10.1140/epjd/e2003-00323-2

THE EUROPEAN PHYSICAL JOURNAL D

Direct experimental characterization of the Bose-Einstein distribution of spatial fluctuations of spontaneous parametric down-conversion

A. Mosset[a], F. Devaux, G. Fanjoux, and E. Lantz

Laboratoire d'Optique P.M. Duffieux, UMR 6603 du CNRS, Université de Franche-Comté, Route de Gray, 25030 Besançon Cedex, France

Received 16 September 2003 / Received in final form 20 November 2003
Published online 6 January 2004 –

Abstract. We present, to the best of our knowledge, the first experimental demonstration by direct detection of the Bose-Einstein photon-number distribution of highly spatially multi-mode but temporally single mode spontaneous parametric down-conversion.

PACS. 42.50.-p Quantum optics – 42.50.Ar Photon statistics and coherence theory – 42.65.-k Nonlinear optics – 42.65.Lm Parametric down conversion and production of entangled photons

1 Introduction

Though it is well-known that the photon-number distribution of incoherent light obeys a Bose-Einstein, or thermal, statistics, it is almost impossible to experimentally distinguish this statistics from a Poissonian distribution in the optical domain for black body sources at usual temperatures. Indeed, the variance of the number n of detected photons (i.e. photo-electrons) reads as [1]:

$$(\Delta n)^2 = \overline{n} + \left(\overline{n}^2/M\right) \tag{1}$$

where $\overline{n}$ is the mean number of detected photons and M, called the degeneracy factor, represents the number (at least one) of spatio-temporal coherence cells, or modes, contained in the detection volume (i.e. the detector area times the detection duration times the light speed). The first term of the right part of equation (1) represents the Poissonian noise, due to the discrete nature of photons. It is present even in absence of intensity fluctuations (case of pure coherent light). The second term comes from the intensity fluctuations of incoherent light. Note that equation (1) is valid for the photo-electrons (pe^-) whatever the quantum efficiency of the detector. However, dividing the photo-electron results by the quantum efficiency in order to retrieve the variance in photons is not allowed, because the Poissonian term is not scale-invariant. For black body radiation at usual temperature in the optical domain, the mean number of photons per mode ($\overline{n}/M$ in Eq. (1)) is far less than one and the Poissonian term dominates in the variance. It can be shown [1] that in this case the Bose-Einstein and the Poissonian statistics are undistinguishable.

On the other hand, cavity-less optical amplification of quantum noise provides incoherent light with many photons per mode. Kravis and Allen [2] experimentally demonstrated 25 years ago that spatial fluctuations of amplified spontaneous emission do obey a Bose-Einstein statistics. In the temporal domain, the same demonstration was made for stimulated Raman scattering [3] and, more recently, for light issued from an erbium amplifier. In the Wong et al. experiment [4], the degeneracy factor was 15 while a very narrow Fabry-Perot filter was used in the Pietralunga et al. experiment [5] in order to obtain a degeneracy parameter as close of one as possible. In both experiments, the fiber optical amplifier ensured a perfect spatial coherence.

In this paper, we experimentally demonstrate by direct detection for one temporal mode the thermal character of statistics of spatial fluctuations of spontaneous down conversion (SPDC), or parametric amplification of quantum noise. Vasilyev et al. [6] studied in the time domain the photon-number distribution of SPDC using a self-homodyne technique of detection. In the spatial domain, spatial fluctuations of SPDC were experimentally investigated by Berzanskis et al. [7] and our group [8] in independent experiments using similar schemes. A semi-quantitative theoretical explanation of these fluctuations was given in [7] and we showed [9] that a semiclassical simulation allows the spatial features (size and shape) of these experimental images to be retrieved. However, the experimental contrast of these spatial fluctuations was lower than that expected by estimating the degeneracy factor. We now attribute this discrepancy to the diffusion of the

[a] e-mail: alexis.mosset@univ-fcomte.fr

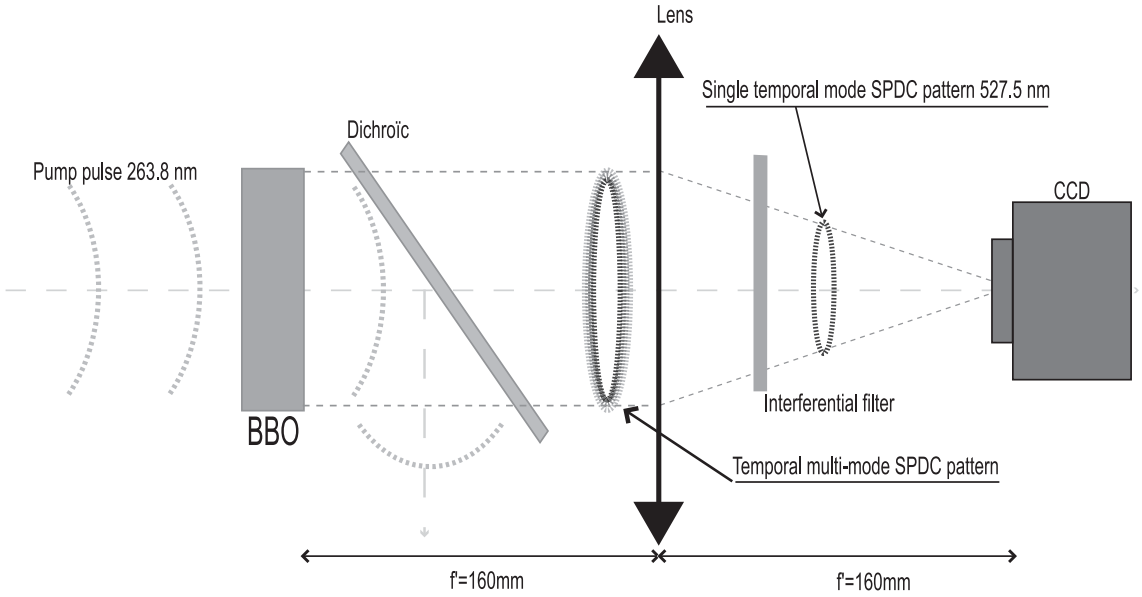

Fig. 1. Experimental set-up.

infra-red SPDC by the silicon sensor of the CCD camera. Therefore, the present experiments are designed in order to generate green light SPDC, at a wavelength where a scientific CCD camera has a good quantum efficiency and, even more importantly, a sharp transfer function of spatial frequencies. Moreover, the reduction of the pulse duration ensures single mode SPDC in the temporal domain. The paper is organized as follows. Section 2 describes the experimental set-up. Section 3 presents the method we have used to calculate a degeneracy factor that takes into account both spatial and temporal modes. In Section 4, we give our experimental results and compare them to spatio-temporal numerical simulations in Section 5. Finally some conclusions and perspectives are summarized in Section 6.

2 Experimental set-up

The experimental set-up is sketched in Figure 1. The pump pulses of 930 fs duration (FWHM), with a time-bandwidth product lower than 0.6, are generated by a frequency-quadrupled Q-switched mode-locked Nd:Glass laser (Twinkle laser by Light Conversion) [10] at a repetition rate of 33 Hz and at a wavelength of 263.75 nm. The collimated pump beam illuminates a 2 mm long BBO crystal and a dichroic mirror separates the UV light from the SPDC beam after the crystal. Because of type I phase matching conditions, the SPDC is generated on a temporal spectrum with a bandwidth of several tens of nanometers [11]. However a narrow interferential filter centered at the parametric degeneracy ($\Delta\lambda = 0.4$ nm at 527.5 nm, transmission coefficient of 60%) is placed before the camera, in order to select an unique temporal mode. This point is critical and we will further discuss in Sections 3 and 5 the number of modes that have to be taken into account. The SPDC pattern is recorded in the far-field on a single-shot, back-illuminated CCD camera from Roper-scientific [12], cooled at -40 °C with a lateral pixel size of 20 μm, a quantum efficiency close to 85% (@527.5 nm), a dark current of 0.03 e^-/pix/s and a read-out noise around 3.4 e^-rms.

3 Estimation of the degeneracy factor

The probability of counting n photo-electrons on a pixel of the camera is given by [13]:

$$P_{(n;\overline{n},M)} = \frac{\Gamma(n+M)}{\Gamma(n+1)\Gamma(M)}(1+M/\overline{n})^{-n}(1+\overline{n}/M)^{-M} \quad (2)$$

where $\Gamma(\xi)$ is the gamma function of argument ξ, and M is the degeneracy factor. This factor, ideally equal to one for an infinitely small pixel and a SPDC beam generated in an unique temporal mode, must take into account the unavoidable departures in the real experiment:

- first, even for a short crystal (2 mm) the dispersion results in a temporal shift between the SPDC generated at the crystal input and the SPDC generated near the crystal output. This shift leads to a stretching of the SPDC pulse, that cannot be strictly temporally single mode, even if the inverse of the bandwidth of the interferential filter is much greater than the duration of the SPDC pulse. Hence a temporal degeneracy factor M_t slightly greater than one must be taken into account;
- second, even if the lateral pixel size is much smaller than the lateral size of a coherence cell in the SPDC beam, the pixels perform some integration between adjacent coherence cells. This phenomenon, spatial analogous of the temporal integration described in [5], has been precisely quantified for classical speckles [14].

The corresponding spatial degeneracy factor M_p is given for square pixels by:

$$M_p = \left\{ \sqrt{\frac{S_c}{S_p}} \mathrm{erf}\left(\sqrt{\frac{\pi S_p}{S_c}}\right) - \left(\frac{S_c}{\pi S_p}\right) \times \left[1 - \exp\left(-\frac{\pi S_p}{S_c}\right)\right] \right\}^{-2} \quad (3)$$

where "erf" represents the error function, S_p is the pixel area and S_c is the coherence area in the far field, proportional to the area of the Fourier transform of the envelope of the SPDC beam recorded at the output face of the crystal. In our experiment, the estimated value of this coherence area is 3.8 pixel areas. This value is obtained by applying the laws of Fourier optics to an experimental image of the Gaussian beam at the crystal output face. With this value, equation (3) gives $M_p = 1.3$;

– finally, we assume that the global degeneracy factor M can be simply estimated as the product of the spatial and the temporal factors:

$$M = M_t M_p. \quad (4)$$

We will show in the following that the temporal M_t factor deduced from the experimental results is in good agreement with spatio-temporal simulations of SPDC.

4 Experimental results

Figure 2 shows an example of a SPDC pattern recorded in the far-field. As in our previous papers [8,9], random fluctuations due to the amplification of quantum noise are clearly visible, with a mean area of the order of the coherence cell area. Unlike in our previous papers, the contrast in Figure 2 is close to one and we show in the following that pixels do exhibit the expected statistics of single mode SPDC. An other important point is the strong correlation between opposite pixels, clearly visible in Figure 2 and already described in references [8,9]. Theory predicts that the statistics on the difference between opposite pixels is sub-Poissonian [15]. Moreover, recent numerical simulations confirm the sub-Poissonian character for realistic situations like Gaussian pump profile [16,17]. However, a quantitative analysis shows that the difference between opposite pixels does not exhibit the sub-shot noise statistics. The reasons are not entirely clear but could reside in some spatial distortions due to the imaging system, especially the interferential filter. To compare the experimental statistics to the theoretical Bose-Einstein distribution, we recorded ten SPDC patterns in the same experimental conditions. The optical axis on each image was determined by using with an appropriate algorithm [18] the symmetrical properties resulting from the signal-idler correlation. By performing the average of all pixels of all images on circles of different diameters, we first verified that phase matching conditions correspond to low-pass filtering and

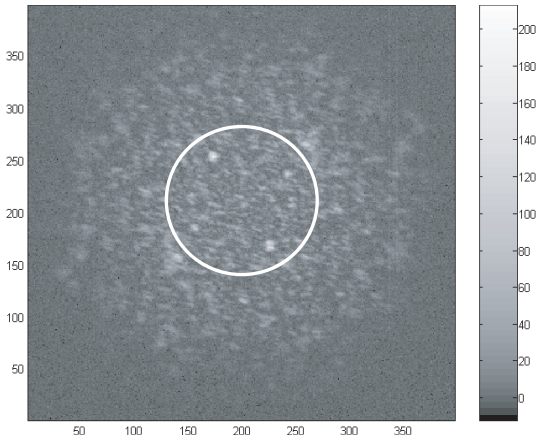

Fig. 2. Far field SPDC pattern recorded on one laser shot. Axes are graduated in pixels. The right scale gives the correspondence between grey-levels and photo-counts.

then selected the pixels inside the drew white circle in Figure 2, for which the statistics appeared to be stationary, i.e. with a negligible gain variation compared to random fluctuations. The radius of the selected area is 70 pixels. The number of independent coherent cells in this area can be assessed as the ratio between the total area and the coherence area, divided by two because of the signal-idler correlation. The result is 2×10^3 independent cells. To deduce the global degeneracy factor M from equation (1) on each image, we must subtract the read-out noise of the camera from the experimental variance:

$$M = \overline{n}^2 / \left((\Delta n)^2 - \overline{n} - (\Delta r)^2\right) \quad (5)$$

where $(\Delta r)^2$ is the variance of the read-out noise, calculated in a small part of the image near the edges, where the incident light is negligible. We find on the ten recorded images an average intensity of $\overline{n} = 12.9\ pe^-/\mathrm{pix}$. The degeneracy factor M obtained by averaging the factors calculated on each image is 1.79 with a standard deviation of $\Delta M = 0.17$. By dividing (see Eq. (4)) this number by the estimated spatial degeneracy factor $M_p = 1.3$ (see Sect. 2), we obtain an estimation of the number of temporal modes of the SPDC beam, $M_t = 1.38$. Figure 3 shows the histogram of the pixels on one image and the theoretical curves corresponding either to a Poissonian or to a Bose-Einstein distribution, calculated with the parameters M and $\overline{n}$ measured on this image. For both theoretical curves, the read-out noise was taken into account by a convolution with a Gaussian distribution. Hence, the distribution of experimental data, including negative intensities due to the subtraction of the average electronic background, is well reproduced by the Bose-Einstein theoretical curve and appears to be very different from a Poissonian distribution. Results with other images are similar. Note however a non negligible difference between the mean degeneracy factors obtained either by averaging the degeneracy factors of each image ($M = 1.79$) or from the histogram of the pixels of all images ($M = 1.62$). A probable cause of this discrepancy is the shot to shot fluctuations of the pump intensity. Indeed, the average of the image strongly

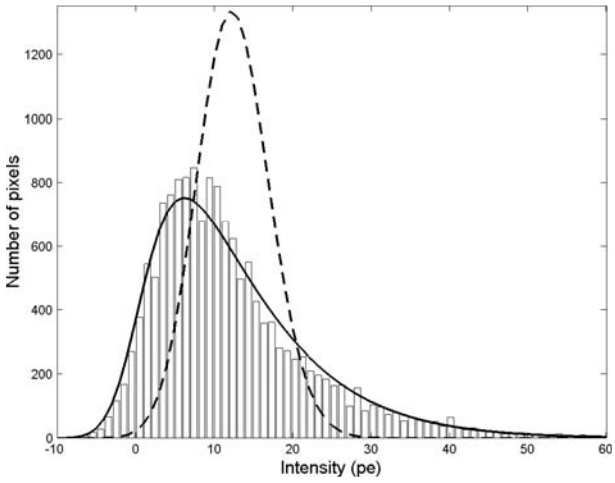

Fig. 3. Histogram of the experimental pixels from one image. Solid line: Bose-Einstein distribution, with the degeneracy factor $M = 1.73$ and the mean $\overline{n} = 12.5$ pe^-/pix calculated on this image. Dashed line: Poissonian distribution with the same mean.

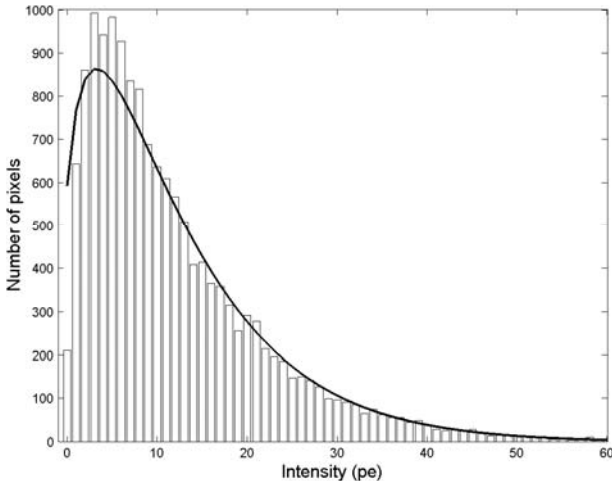

Fig. 4. Histogram of the numerical simulation with $\overline{n} = 12.2$ pe^-/pix and corresponding theoretical curve.

Table 1. Evolution of the M_t factor according to average intensity of SPDC in pe^-/pix.

$\overline{n}$	9.9	12.2	14.9	18.2	22	1.2×10^8
M_t	1.50	1.44	1.42	1.37	1.36	1.10

varies from one shot to another, more than expected for purely random fluctuations of a Bose-Einstein distribution with constant parameters.

5 Numerical simulations

We have recently extended our semiclassical simulation of SPDC by adding one temporal dimension to the 2D spatial model of reference [9]. The complete description of this simulation will be published elsewhere [19]. To study the temporal walk-off effect, we performed numerical simulations for different crystal lengths and verified that the contrast decreases when increasing the crystal length. Indeed, for long crystals, the SPDC generated at the beginning of the crystal is temporally shifted, because of dispersion, with respect to the pump pulse near the crystal output face. Hence, the SPDC generated near the output face is almost not correlated with the earlier generated parametric fluorescence and the global SPDC is not temporally single mode. Next we studied the impact of the gain level on the number of temporal modes for a 2 mm long crystal. Results are given in Table 1. Because the global experimental quantum efficiency of the imaging system formed by the detector, the interferential filter and the lens is estimated to be 0.51, the results in photo-electrons are obtained as follows. First, the spatio-temporal simulation of SPDC provides an intensity, that is converted in photons after temporal and spatial integration on a pixel. Then, these photons are randomly destroyed, with a probability of 0.49, in order to conserve a Poissonian noise for the retrieved photo-electrons (a simple multiplication would give a wrong sub-Poissonian statistics). Finally the number of temporal modes is calculated using equation (5), with no read-out noise.

An interpolation of Table 1 leads to $M_t \approx 1.43$ for the experimental mean $\overline{n} = 12.9$ pe^-/pix. This result is in good agreement with the number of temporal modes estimated from the experimental images ($M_t = 1.38$). We verify also that for a very high gain ($\overline{n} = 1.2 \times 10^8$ pe^-/pix) the number of temporal modes becomes close to one. The estimation of the global quantum efficiency of the imaging system appears to be among the main sources of uncertainties. Figure 4 presents the histogram of the pixels issued from the simulation that gives a mean number $\overline{n} = 12.2$ pe^-/pix, giving $M_t = 1.44$. The corresponding theoretical curve is also drew in the figure. The horizontal scale starts exactly from zero because electronic background corrections are not necessary in numerical simulations. Note also that there is no influence of the pixel area (M_p factor = 1), because quantum noise is itself simulated pixel by pixel. For higher gains, the M_t factor decreases, as shown in Table 1. Indeed, the SPDC beam becomes temporally very narrow, because of exponential amplification, while the frequency bandwidth remains fixed by the interferential filter.

6 Conclusion

We have experimentally demonstrated that spatial fluctuations of spontaneous down conversion obey an almost non degenerate Bose-Einstein statistics, for sufficiently small pixels and short pulses. The considered fluctuations are purely spatial because all statistical quantities (variance, degeneracy factor...) are computed on one image, and not from the fluctuations between different shots. Moreover, we observed strong correlations between opposite points corresponding to signal-idler entanglement. However, the quantitative values remained in the classical domain while theory predicts sub-shot-noise correlation.

While experiments in Como (group of prof. Di Trapani) are designed to demonstrate this sub shot-noise correlation in a type 2 configuration [20], the present experiment should, in principle, lead to the result for a type 1 crystal, after the solution of some not completely clear experimental problems.

This work has been supported by the European Union in the frame of the QUANTIM network (contract IST 2000-26019).

References

1. J.W. Goodman, *Statistical Optics* (Wiley Classics Library, New York, 2000), pp. 481-490
2. S.P. Kravis, L. Allen, Opt. Comm. **23**, 289 (1977)
3. I.A. Walmsley, M.G. Raymer, Phys. Rev. Lett. **50**, 962 (1983)
4. W.S. Wong, H. Haus, L.A. Jiang, P.B. Hansen, M. Margalit, Opt. Lett. **23**, 1832 (1998)
5. S.M. Pietralunga, P. Martelli, M. Martinelli, Opt. Lett. **28**, 152 (2003)
6. M. Vasilyev, S.-K. Choi, P. Kumar, G.M. D'Ariano, Optt. Lett. **23**, 1393 (1998)
7. A. Berzanskis, W. Chinaglia, L.A. Lugiato, K.-H. Feller, P. Di Trapani, Phys. Rev. A **60**, 1626 (1999)
8. F. Devaux, E. Lantz, Eur. Phys. J. D **8**, 117 (2000)
9. E. Lantz, F. Devaux, Eur. Phys. J. D **17**, 93 (2001)
10. `http://www.lightcon.com/`
11. F. Devaux, E. Lantz, J. Opt. Soc. Am. B **12**, 2245 (1995)
12. `http://www.roperscientific.com/`
13. J.W. Goodman, *Statistical Optics* (Wiley Classics Library, New York, 2000), pp. 475-479
14. J.W. Goodman, *Laser speckle and related phenomena* (Dainty, Springer-Verlag, 1984), Chap. 2, p. 51
15. A. Gatti, E. Brambilla, L.A. Lugiato, M.I. Kolobov, Phys. Rev. Lett. **83**, 1763 (1999)
16. E. Lantz, N. Treps, C. Fabre, E. Brambilla, Eur. Phys. J. D (submitted)
17. E. Brambilla, A. Gatti, M. Bache, L.A. Lugiato, Phys. Rev. A (accepted)
18. L. Oriat, E. Lantz, Patt. Recogn. **31**, 761 (1998)
19. G. Fanjoux, F. Devaux, E. Lantz, H. Maillotte, submitted
20. O. Jedrkiewicz, Y. Jiang, P. Di Trapani, E. Brambilla, A. Gatti, L.A. Lugiato, EH5-4-THU, CLEO/EQEC 2003, 22-27 June 2003, Munich (D)